UNIVERSIDAD NACIONAL DE COLOMBIA
SEDE MEDELLÍN
FACULTAD DE MINAS

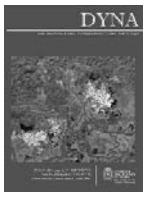

DYNA
http://dyna.medellin.unal.edu.co/

Theoretical and experimental study of the electronic, crystalline, morphologic, compositional, magnetic and dielectric properties of the Sr_2DyNbO_6 material

Ramiro Cardona, David A. Landínez-Téllez & Jairo Roa-Rojas

Grupo de Física de Nuevos Materiales, Departamento de Física, Universidad Nacional de Colombia, Bogotá D.C., Colombia. rcardonac@unal.edu.co, dalandinezt@unal.edu.co, jroar@unal.edu.co

Received: February 12th, 2016. Received in revised form: November 12th 2016. Accepted: January 30th, 2017.

Abstract
We report experimental and theoretical results of crystal structure, morphology, magnetic and electric features, and electronic structure for the Sr_2DyNbO_6 ceramic compound. Samples were produced by the solid-state reaction recipe. X-ray diffraction experiments show that the material crystallizes in a monoclinic structure, $P2_1/n$ space group. SEM images exhibit a granular submicrometric surface. Temperature curves of magnetic susceptibility reveal a paramagnetic response. Curie law fitting permitted to obtain a magnetic moment 10.28 μ_B. Polarization as a function of electric fields shows a hysteretic feature with 264.28 relative dielectric constant at 300 K. DFT calculations of electronic structure suggest the semiconductor character of this material, energy gap 3.21 eV for the spin-up polarization and 0.26 eV for spin-down. The calculated effective magnetic moment was 10.0 μ_B, which is strongly in accordance with the measured value. The theoretical cell parameters obtained from the Murnaghan state-equation are 98.5% in agreement with the experimental result.

Keywords: Complex perovskite; magnetic properties; electronic structure.

Estudio teórico y experimental de las propiedades electrónicas, cristalinas, morfológicas, composicionales, magnéticas y dieléctricas del material Sr_2DyNbO_6

Resumen
Se reportan resultados experimentales y teóricos de estructura cristalina, morfología, carácter magnético y eléctrico, y estructura electrónica para el material cerámico Sr_2DyNbO_6. Las muestras fueron producidas mediante reacción sólida. Resultados de difracción de rayos X muestran que el material cristaliza en una estructura monoclínica, grupo espacial $P2_1/n$. Imágenes de MEB muestran superficies granulares submicrométricas. La susceptibilidad en función de la temperatura revela una respuesta paramagnética con momento magnético 10.28 μ_B. La histéresis de polarización en función del campo eléctrico a *300K* permitió obtener una constante dieléctrica de 264.28. Cálculos de estructura electrónica por DFT sugieren que el material es semiconductor con brecha de energía 3.21 eV para la orientación espín arriba y 0.26 eV para espín abajo. El momento magnético calculado es 10.0 μ_B, muy próximo del valor medido. Los parámetros de red obtenidos mediante la ecuación de Murnaghan están de acuerdo con los resultados experimentales en un 98.5%.

Palabras clave: Perovskita compleja; propiedades magnéticas; estructura electrónica.

1. Introduction

Ceramic materials known as perovskites are recognized by the combination of metal with non-metallic elements. The atomic arrangement in the mineral can be described as a FCC packing of metal cations A and anions X with a small metal

How to cite: Cardona, R., Landínez-Téllez, D.A. and Roa-Rojas, J., Theoretical and experimental study of the electronic, crystalline, morphologic, compositional, magnetic and dielectric properties of the Sr2DyNbO6 material. DYNA 84(201), pp. 88-94, 2017.

© The author; licensee Universidad Nacional de Colombia.

cation B occupying octahedral sites generated by the anions. Based on this description, the ideal perovskite materials are usually depicted as ABX_3 in a cubic cell, in whose center is placed the cation A; cations B occupy the eight corners and anions X occupy the midpoints between cations B [1]. Ideal perovskites are insulators and, as the three axes of the cube are identical, have isotropy of the electrical, optical and mechanical properties. In many perovskites, however, distortions are observed because there are differences among the ionic radius of A and B cations, which causes the anions X and cations B move, giving rise to rotations and inclinations of the octahedral coordination. The unit cell can be modified through partial substitution of cations B to give rise to double perovskites of $A_2BB'X_6$ type [2]. Commonly position A is occupied by rare earth, alkaline earth or alkali; the B and B' positions are occupied usually by transition metals and X is oxygen, giving rise to a large number of possible combinations associated with different physical properties ranging from ferroelectric insulators [3], magnetoresistive and ferromagnetic [4], halfmetallics [5] to multiferroics [6]. Previous researches have shown that the Sr_2RESbO_6 (RE=Dy, Ho, Gd) double perovskite crystallize in FCC lattices with geometrical frustration [7]. Other authors report that the RE^{3+} and Sb^{5+} cations adopt an ordered arrangement in the double-perovskite structure with alternated octahedral. In the case of RE=Dy, they have observed frustrated magnetic ordering. The aim of this work is to study the effect of the introduction of Nb^{5+} in the structural site of the Sb^{5+} on the crystal cell and the magnetic and electric responses. The starting point for the work done is the synthesis of the material through standard methods for the perovskite family of compounds, experimentally studying the structural, electrical and magnetic responses, and theoretically predicting the electronic properties in the vicinity of the Fermi level.

2. Experimental Setup

In order to prepare Sr_2DyNbO_6 samples, oxide precursor powder of $SrCO_3$, Dy_2O_3 and Nb_2O_5, from Aldrich, having a purity of 99.9%, were solid-reacted at a temperature of 900 ºC for 12 h after being carefully ground in an agate mortar for 3 h and pelletized to form discs of 9.00 mm diameter. Subsequently, samples were pulverized for an hour, pressed in tablet form, and sintered at 1350 °C for 36 h. The diffraction patterns were obtained on a Panalytical X'Pert Pro MPD, which has a radiation source with wavelength $\lambda_{CuK\alpha}$=1.54064 Å, a step of 0.02 degrees and exposure time of 5 s. Rietveld refinement of the experimental data was carried out using the GSAS program [8]. Measurements of magnetic susceptibility as a function of temperature were performed by means VersaLab equipment produced by Quantum Design. A VEGA3 TESCAN electronic microscope was used in order to examine the surface morphology of samples. Polarization curves as a function of electric field were measured by the utilization of a Ferroelectric Tester (Radiant Technologies) on the presence of high voltages.

3. Calculation method

In order to determine both the band and electronic structures of the Sr_2DyNbO_6 ceramic, the method Full-Potential Linear Augmented Plane Wave method (FP-LAPW) was implemented by considering the Kohn-Sham Density Functional Theory (DFT) [9], for which the Generalized Gradient Approximation (GGA) was adopted, and considering the exchange correlation energy predicted by Perdew, Burke and Ernzerhof [10]. The calculating self-consistency was carried out through the Wien2k numeric package [11]. Theoretical calculations of the structural parameters of the material were made through the minimization of the energy as a function of the volume of the unit cell, with a corresponding fitting to the Murnaghan's state equation [12]. Then, the bulk modulus, the minimum energy value and the equilibrium lattice parameters and associated volume were obtained. The muffin-tin radii introduced for the calculations were R_{Sr}=1.25415 Å, R_{Dy}=1.25415 Å, R_{Nb}=1.04777 Å, and R_O=0.94194 Å, with an angular momentum inside the muffin-tin sphere up to l =10, a k_{max}=250 points in the irreducible Brillouin zone and G_{max} =12.0, RMT*K_{max} = 7.0 (maximum vector in the momenta space). At last, for the self-consistent calculation, total energies of 0.0001 Ry, charge of $5.3x10^{-5}$ Å and internal forces of 1.0 mRy/u were taken in to account.

4. Results and discussion

XRD pattern for the Sr_2DyNbO_6 material is presented in Fig.1. The strong peaks observed in the diffractogram have the signature that characterizes a superstructure of the perovskite type. These are characteristics of a primitive perovskite plus a few weak line diffractions arising from the superlattice. From the GSAS Rietveld refinement it was obtained that the respective structure corresponds to a monoclinic double perovskite, which belongs to the $P2_1/n$ (#14) space group.

The particular feature of this primitive cell is the occurrence of which denotes one 180º rotation around a screw axis, with a subsequent translation in the [010] direction at the half lattice parameter, and a final diffraction perpendicular to the [010] direction respect to a sliding crystallographic plane. As a direct result of the Rietveld refinement is the cell parameters of the studied perovskite were *a*=5.7314 Å, *b*=5.9054 Å and *c*=8.2222 Å. It is known

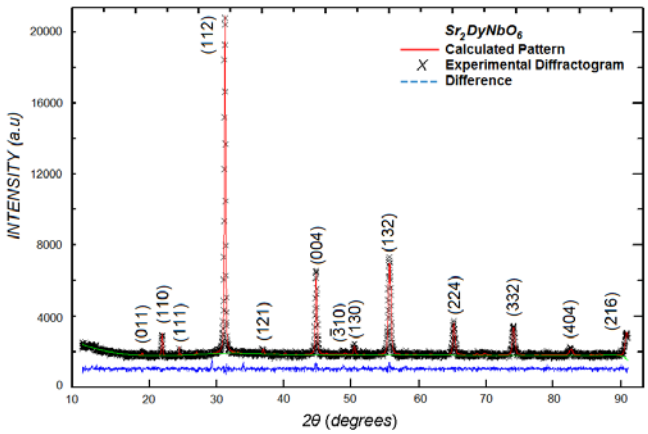

Figure 1. Characteristic XRD pattern for the Sr_2DyNbO_6 complex perovskite. Index for the respective reflective planes are indicated in the picture.Source: The authors.

that in the ideal ABO_3 single perovskite the bigger cation A is 12-coordinated with the O anions while the smaller cation B has an octahedral 6-coordination with the neighborhood of O anions. Double perovskites with mixed B, B' are usually characterized by a larger unit cell represented through the formula $A_2BB'O_6$ [13]. As showed in the structure of Fig. 2, there are evidences of distortion of the DyO_6 and NbO_6 octahedral from the ideal symmetrical cube. In the bc-plane showed in Fig. 2a, tilt angle of octahedral η=15.83º is observed and in the ac-plane of Fig. 2b the tilt angle ρ=18.14º is evident. The monoclinic angle is calculated to be β=90.0276º.

The monoclinic structure belonging to the $P2_1/n$ (#14) space group is determined by the following details: peaks (011) and (111) appear in the pattern; diffractions (240), (004) and (404) are indicative of in-phase tilting (*ood*); peak (330) in the pattern shows the occurrence of atomic displacements (*ddo*); and peaks (011), (111) and (3-10) reveal the ordered arrangement of cations forming super-structure diffractions (*ooo*), which suggest simultaneously the appearance of in-phase and out-of-phase tilting [14]. The Dy^{3+} and Nb^{5+} are located on the 2d and 2c Wyckoff positions (see Table 1) make up two DyO_6 and NbO_6 octahedral alternatively arrangement in two subsequent fcc subcells. On the other hand, 1,2 and 3 Oxygen anions are sited in the octahedral corners and the Sr^{2+} cation is localized in the A-site of the generic $A_2BB'O_6$ structure, in the cavities generated by the corners that are shared by the DyO_6 and NbO_6 octahedral. As presented in Table 1 and observed in Fig. 2c, Sr^{2+} cation occupies the 4e Wyckoff position 4e.

These mismatches give rise to rotations of the DyO_6 and NbO_6 octahedral and shifts of Sr cations and O ions that rotate the structure to fix the Dy^{3+} and Nb^{5+}-cations on the B and B' sites of the double perovskite, besides, the small size of the Sr cation produces a large distortion from the ideal cubic symmetry. Consequently, the DyO_6 and NbO_6 octahedral are forced to maintain the union between their corners, while supporting the tilting between them. To find the mismatch between the Sr–O, Dy–O and Nb–O inter-atomic bond lengths we calculated the tolerance factor τ defined by the ratio

$$\tau = \frac{r_A + r_O}{\sqrt{2}\left(\frac{r_B + r_{B'}}{2} + r_O\right)}, \quad (1)$$

where r_A, r_B, $r_{B'}$ and r_O are the ionic radius of the A, B, B' and O-ions, respectively. The calculated tolerance factor for the Sr_2DyNbO_6 perovskite was τ=0,9285. This value suggests a rock-salt arrangement over the two non-equivalent DyO_6 and NbO_6 octahedral sites. The distances between the Dy-O, Nb-O and Sr-O ions are not always the same, which justifies a tolerance factor less than unity with distortions of octahedral. These distortions are also identified through η and ρ angles.

The Secondary Electrons Image of SEM of Fig. 3 for the Sr_2DyNbO_6 reveals a qualitative approximation to the surface microstructure. Strongly coupled particles are observed in the surface morphology, which is a characteristic of good sinterization in the polycrystalline sample. Picture evidences the formation of micrometric clusters of nanometric grains.

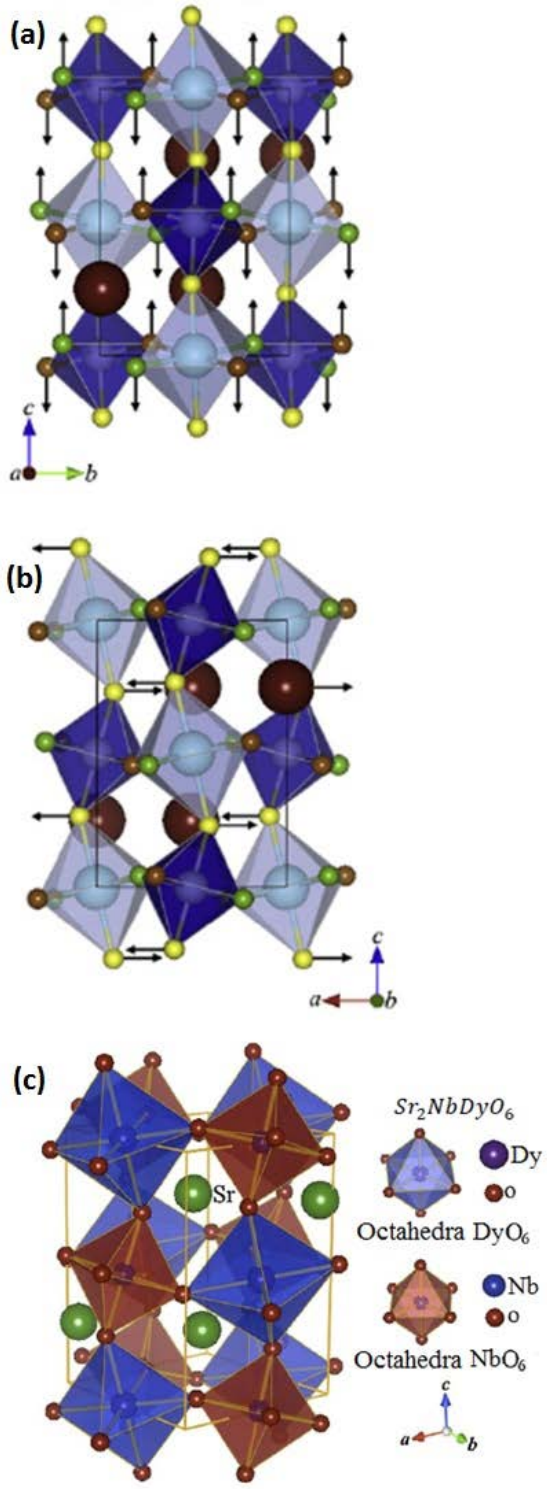

Figure 2. Crystalline structure of the Sr_2DyNbO_6 monoclinic perovskite. (a) bc-plane, (b) ac-plane and (c) 3D-structure.
Source: The Authors

The discrepancy between the ionic radii of all cations and oxygen is one of the reasons why the double perovskite Sr_2DyNbO_6 is distorted from the ideal cubic $A_2BB'O_6$ structure.
Table 1.

Atomic positions of cations and anions on the unit cell of Sr2DyNbO6, obtained from the Rietveld refinement.

Atom	Wyckoff Site	*x*	*y*	*z*
Sr^{2+}	*4e*	0.5165	0.5490	0.2483
Dy^{3+}	*2c*	0.0000	0.5000	0.0000
Nb^{5+}	*2d*	0.5000	0.0000	0.0000
$O^{2-}(1)$	*4e*	0.2241	0.1917	-0.0439
$O^{2-}(2)$	*4e*	0.3119	0.7257	-0.0439
$O^{2-}(3)$	*4e*	0.4122	-0.0135	0.2325

Source: The Authors.

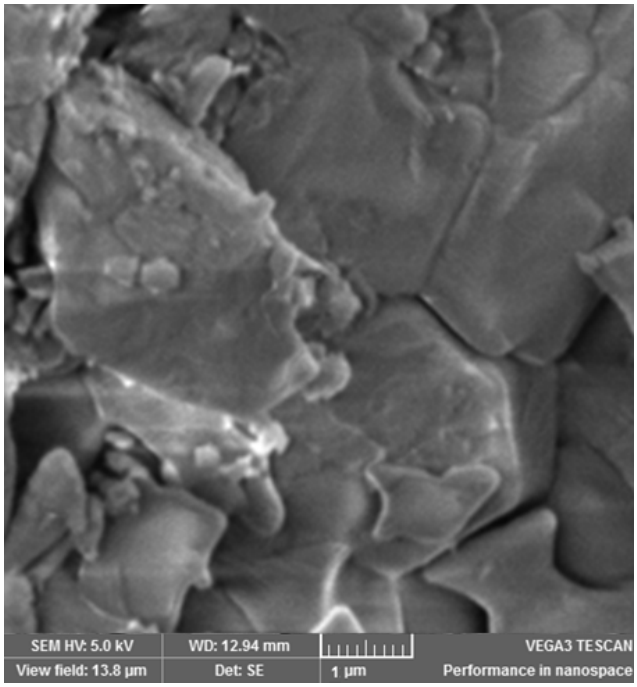

Figure 3. Scanning Electron Microscopy image for the Sr_2DyNbO_6 complex perovskite.
Source: The Authors

In order to determine the mean grain size, we use the intercept method drawing random straight lines across the micrograph. Then, we perform a counting of the number of grain boundaries intersecting the line. At last, the mean grain size is found by dividing the number of intersections by the line length. The accuracy depends on the scale and magnification micrograph applied in the spread of experimental error. It is clear that the grains could end up having a few tens of *nm*, forming groups, which have appearance of clusters of several μm sizes. The particle size D was calculated using the Scherrer equation, which is based on widening of maximum intensity weak of the XRD pattern due to particle size exclusively, and defined by the ratio $D=K\lambda/\beta(\theta)\cos\theta$, where K is a constant, λ =0.15406 nm is the radiation length and $\beta(\theta)=\Delta(2\theta)$ represents the half-widening of profile [15]. The calculated particle size for the Sr_2DyNbO_6 is D=42.5 nm. As D depends on the nucleation and growth rate, then, the value obtained for the Sr_2DyNbO_6 material is attributed to the decomposition reaction toward oxides, which may be responsible of the particle size D [13]. Because the solid-state reaction destroys the original morphologies of the precursor oxides, fine particles with similar size distributions can be obtained. These fine particles might be combined once and again to form agglomerates with size distributions like that shown in Fig. 3. Since, the increase of the annealing temperature or the sintering time the particle size D of material also increases, and then the grain morphology changes from the common plate-like form observed in ceramics, toward a spherical-like form. These phenomena produce a decreasing in surface tension and lead to a transformation of the crystallographic structure toward a low symmetric $P2_1/n$. The crystal structure of the Sr_2DyNbO_6 suffers a decrease of the lattice parameters and consequently the unit cell volume decreases as D increases; this could be due to decreasing of the ratio of surface to volume with the D increases [13]. This result suggests that for D=42.5 nm at 1350 K, the crystal structure of the Sr_2DyNbO_6 suffers grain size-induced polarization rotation, which produces a phase transition toward monoclinic $P2_1/n$ (#14) phase as the particle size D increases. Besides, the particle size D obtained for the Sr_2DyNbO_6 morphology suggests that the influence of the sliding processes decreases as D increases and ceramic samples with small D suffer large amount of grain boundaries, which are responsible for sliding processes.

The magnetic response of Sr_2DyNbO_6 has been investigated by measuring the DC magnetic susceptibility in the temperature range 50 to 300 K on the application of H=10 Oe magnetic field intensity. Fig. 4 shows the temperature dependence of the DC magnetic susceptibility for Sr_2DyNbO_6.

The magnetic susceptibility data of this picture can be fitted well with the Curie law $\chi=\chi_0+C/(T-\theta_c)$, where $C=N\mu^2_{eff}/3k_B$ is the Curie constant, N represents the Avogadros's number, μ_{eff} is the effective magnetic moment ($\mu_{eff}=P_{eff}\mu_B$), P_{eff} represents the effective Bohr magneton number, μ_B is the Bohr magneton, K_B is the Boltzmann constant, θ_c is the paramagnetic Curie temperature and χ_0 is the temperature independent susceptibility term. The value of the temperature independent susceptibility term is χ_o = 0.00812 emu/mol.Oe. The Curie constant, estimated from the

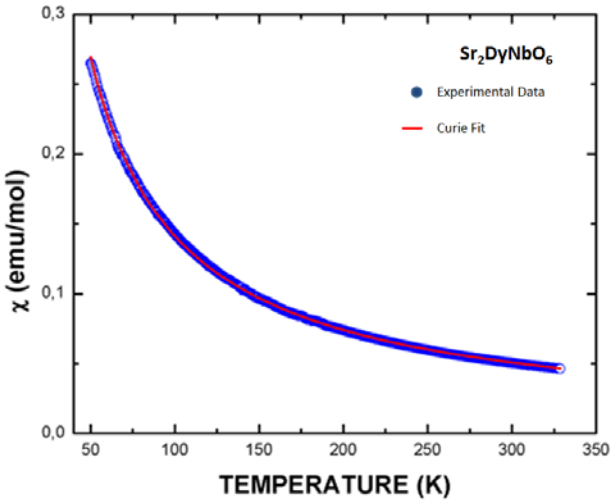

Figure 4. Magnetic susceptibility curve as a function of temperature and Curie fitting for the Sr_2DyNbO_6 double perovskite.
Source: The Authors.

fitting in Fig. 4 is C=13.2423 emu.K/mol.Oe. The effective magnetic moment due the Dy^{3+} ion, calculated from the Curie constant is μ_{eff}=10.28 μ_B. This value corresponds 96.7% with the expected $P_{eff}=g[J(J+1)]^{½}$=10,63 for an isolated Dy^{+3} cation with configuration $4f^{10}5d^{0}6s^{2}$, calculated by the Hund's rules, where g represents the Landé factor and J is the quantic number [16]. This difference may be attributed to the crystal field effects of the trivalent Dy^{+3} cation, which explain the magnetic susceptibility in Sr_2DyNbO_6.

Fig. 5 shows the hysteric behavior of the electric polarization on the application of electric fields up to 3.0 kV/cm. The characteristic curve reveals strong dielectric loss with a saturation polarization of 0.065 μc/cm^2, remnant polarization of 0.039 μc/cm^2 and coercive fields of 1.48 kV/cm.

From the estimate values of the P_S, we determine the capacitance of the Sr_2DyNbO_6 material, through the equation $P_s=(C/A)V$, where A represents the area of the sample, V is the applied voltage and C is the capacitance. Then, we obtain C/A as the slope in a picture of saturation polarization as a function of voltage. The electric permittivity is calculated by the expression $\varepsilon=(C/A)(d/\varepsilon_0)$, where d represents the distance between the capacitor plates and ε_0 is the electric permittivity in vacuum [17]. The saturation of polarization in the dielectric hysteresis curve permitted determine the relative dielectric constant at room temperature ε=264.28, which is an appropriate value for microwave applications**.**

Calculations of minimization of energy as a function of volume by the GGA approximation, for the space group $P2_1/n$ (#14), produce the points of Fig. 6. The theoretical points were fitted by the Murnaghan's state equation [12]. In the picture the minimum energy value is obtained for 0.0734 eV. The equilibrium volume is 290.8125 Å^3, which corresponds with lattice constants a=5.8161 Å, b=5.9927 Å and c=8.3437 Å, with a monoclinic angle β=90.0276º and a volume modulus Bo=148.93 GPa. The lattice parameters obtained from the experimental results are ~ 98.5% in agreement with those obtained from the GGA approximation.

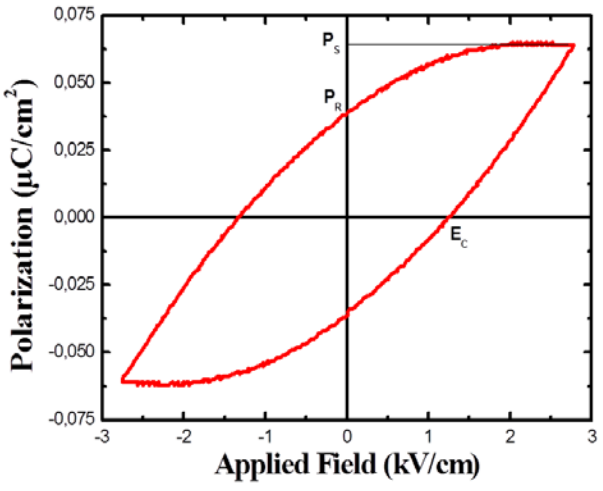

Figure 5. Hysteresis curve of polarization as a function of the electric applied field measured in the Sr_2DyNbO_6 material. Saturation and remnant polarizations and coercive field is signaled in the figure.
Source: The Authors.

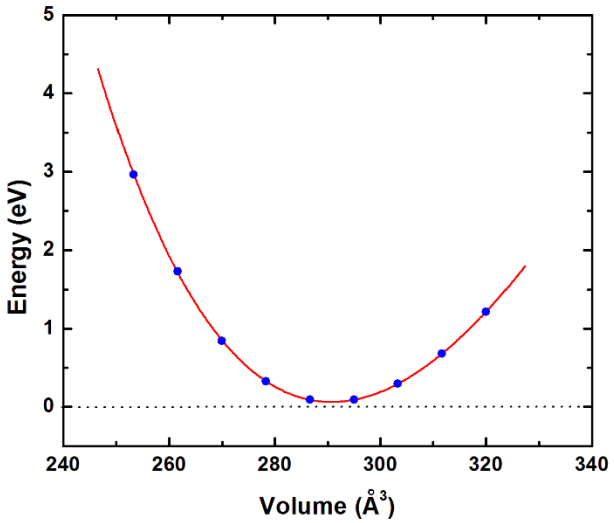

Figure 6. Curve of minimizations of energy as a function the unit cell volume.
Source: The Authors.

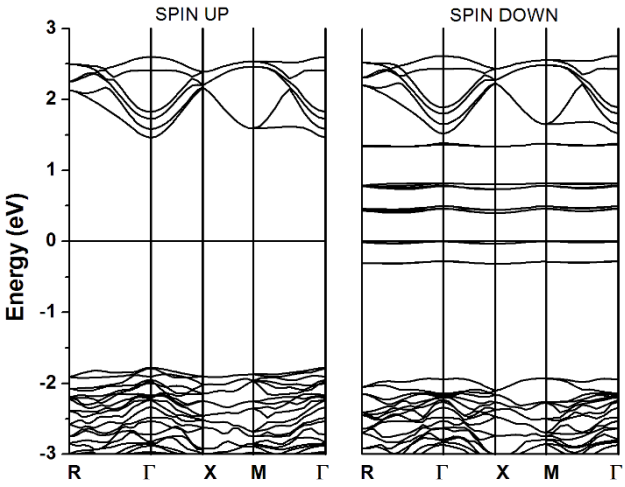

Figure 7. Band structure with spin polarization calculated for the Sr_2DyNbO_6 material.
Source: The Authors.

Fig. 7 exemplifies the band structure calculated for the Sr_2DyNbO_6 material by considering spin polarization. In the picture, the Fermi level is assigned to E=0.

For the spin up orientation an insulator character is observed with gap energy from -1.75 eV to 1.45 eV (E_g=3.21 eV), while for the spin down polarization E_g=0.26 eV and five group of localized bands are identified in the energy regime from -1.85 eV to 1.05 eV. These exotic bands correspond to the $4d^4$ orbital of Nb.

Fig. 8 represents Total and Partial density of states (DOS) for both up and down spin orientations. In the valence band majority states are located far the Fermi level, in the energy interval between -5.8 eV and -1.8 eV. From the Fig. 8 it is clear that the predominant contribution to the DOS for the up configurations is due to $4d^4$ states of Nb. Representative participation of $2p^4$ oxygen orbitals for the up and down orientations are observed in this energy region. Contributions due to $4f^{10}$ states of Dy and

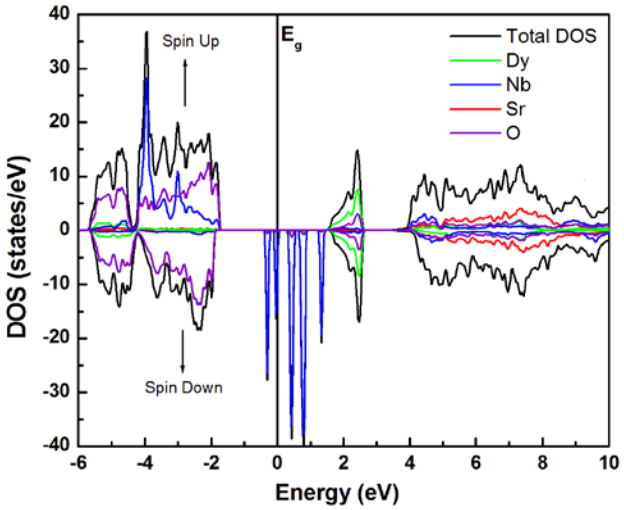

Figure 8. Total and partial DOS for both up and down spin polarization calculated for the Sr_2DyNbO_6 perovskite.
Source: The Authors.

$5s^2$ of Sr are very incipient. Close to the Fermi level, between -0.50 eV and 0 eV, strong contribution of $4d^4$ Nb-states clearly appears in the valence band. Close to the Fermi level in the conduction band, three isolated and localized contributions of the $4d^4$ orbital of Nb are observed for the spin down orientation. These are responsible for the semiconducting behavior in this spin channel.

On the other hand, in the energy regime from 1.53 eV to 2.62 eV a symmetric-like feature of the spin up and spin down DOS is observed with representative contributions of the 4f10 and 2p4 states of Dy and O, respectively. Far the Fermi level, above 3.79 eV, 5s2-Sr states and other incipient orbital are available. In Fig. 8 is possible to observe an apparent conductor character in the DOS for the spin down orientation, but it is important to clarify that this effect is due to the underestimation of the gap which is characteristic of the Wien2k package. Magnetic moment of mixed charge density was calculated from the asymmetry of the Dy-4f states close the Fermi level. Total magnetic moment in cell was determined to be 10.0 μB for Sr2DyNbO6. This result is 97.3% in agreement with the experimental obtained value.

5. Conclusions

GSAS refinement of experimental XRD data of Sr_2DyNbO_6 synthesized by the solid state reaction method reveals the monoclinic structure of this double perovskite material, space group $P2_1/n$ (#14). Nanometric grains (42.5 nm) distributed in micrometric clusters were observed in SEM images. Curie fitting in the paramagnetic regime permitted to determine the effective magnetic moment μ_{eff}=10.28 μ_B. This value is close to the theoretical predicted by the Hund's rules. Measurements of polarization as a function of applied electric fields reveal the strongly dielectric feature of the material. From the polarization saturation the relative dielectric constant was determined to be ε=264.28. Crystallographic parameters were obtained from adjustment of minimal energy with the Murnaghan state equation taking in to account the $P2_1/n$ space group. These are 98.5% in accordance with the experimental lattice parameters. The obtained volume modulus Bo=148.93 GPa is typical of the double perovskite-like materials [18]. Calculation of band structure and DOS with spin polarization predicts the insulator behavior (E_g=3.21 eV) of the Sr_2DyNbO_6 for the spin up orientation and semiconductor (E_g=0.26 eV) for the other. Major contributions to the DOS close to the Fermi level are attributed to the $4d^4$-Nb states. The calculated effective magnetic moment is 97.3% in agreement with the experimental value.

Acknowledgments

This work was partially supported by the División de Investigaciones Sede Bogotá (DIB) of Universidad Nacional de Colombia.

References

[1] Lu, X., Xie, J., Shu, H., Liu, J., Yin, C. and Lin, J., Microwave-assisted synthesis of nanocrystalline $YFeO_3$ and study of its photoactivity, Materials Science and Engineering B, Solid-State Materials for Advanced Technology, 138(3), pp. 289-292, 2007, DOI: 10.1016/j.mseb.2007.01.003

[2] Landínez-Téllez, D.A., Deluque-Toro, C.E. and Roa-Rojas, J., Electronic, structural and ferroelectric properties of the Ba_2ZrTiO_6 double perovskite, DYNA, 81(183), pp.126-131, 2014. DOI: 10.15446/dyna.v81n183.34859

[3] Masud, Md.G., Sakata, H., Biswal, A.K., Vishwakarma, P.N. and Chaudhuri, B.K., Structural, ac conductivity scaling and magnetodielectric behaviour of a partially disordered insulating ferromagnetic double perovskite Eu_2NiMnO_6, J. of Phys. D: Appl. Phys. 48(37), 375504, 2015, DOI: 10.1088/0022-3727/48/37/375504.

[4] Maignan, A., Raveau, B., Martin, C. and Hervieu, M., Large intragrain magnetoresistance above room temperature in the double perovskite Ba_2FeMoO_6, J. Solid State Chem. 144(1), pp. 224-227, 1999, DOI: 10.1006/jssc.1998.8129.

[5] Weng, K.C. and Wang, Y.K., Half-metallic antiferromagnetism in double perovskite $BiPbCrCuO_6$, J. Appl. Phys. 117(17), 17D716, 2015. DOI: 10.1063/1.4916758.

[6] Landínez-Téllez, D.A., Peña-Rodríguez, G., Fajardo, F., Rodríguez J.A., and Roa-Rojas, J., Structural, magnetic, multiferroic, and electronic properties of Sr_2TiMnO_6 double perovskite, DYNA 79(171), pp. 111-115, 2012.

[7] Karunadasa, H., Huang, Q., Ueland, B.G., Schiffer, P. and Cava, R.J., Ba_2LnSbO_6 and Sr_2LnSbO_6 (Ln = Dy, Ho, Gd) double perovskites: Lanthanides in the geometrically frustrating fcc lattice., Proc. Natl. Acad. Sci. USA, 100(14), pp. 8097-80102, 2003, DOI: 10.1073/pnas.0832394100.

[8] Larson, A.C. and Von Dreele R.B., General structure analysis system (GSAS), Los Alamos National Laboratory Report - LAUR, 2000, pp. 86-748.

[9] Khon, W. and Sham, L.S., Self-Consistent equations including exchange and correlation effects. Phys. Rev., 140(4A), pp. A1133-A1138, 1965, DOI: 10.1103/PhysRev.140.A1133.

[10] Perdew, J.P., Burke, K. and Ernzerhof, M., Generalized gradient approximation made simple, Phys. Rev. Lett., 77(18), pp. 3865-3868, 1996, DOI: 10.1103/PhysRevLett.78.1396.

[11] Blaha, P., Schwarz, K., Madsen, G.K.H., Kvasnicka, D. and Luitz, J., WIEN2k, An Aug-mented Plane Wave + Local Orbitals Program for Calculating Crystal Properties. Karlheinz Schwarz, Techn. UniversitÄat Wien, Austria, 2001. ISBN 3-9501031-1-2.

[12] Murnaghan, F.D., The compressibility of media under extreme pressures, Proc. Natl. Acad. Sci. USA, 30(9), pp. 244-247, 1944. DOI: 10.1073/pnas.30.9.244

[13] Triana, C.A., Landínez-Téllez, D.A., Rodríguez, J.A., Fajardo, F. and Roa-Rojas, J., Electronic, crystal structure and morphological

properties of the Sr_2DyRuO_6 double perovskite, Materials Letters, 82(1), pp. 116-119, 2012, DOI: 10.1016/j.matlet.2012.05.041.
[14] Triana, C.A., Corredor, L.T., Landínez Téllez, D.A. and Roa-Rojas, J., High temperature-induced phase transitions in Sr_2GdRuO_6 complex perovskite, Mater. Res. Bull., 46(12), pp. 2478-2483, 2011, DOI: 10.1016/j.materresbull.2011.08.024.
[15] Patterson, A., The Scherrer formula for X-Ray particle size determination, Phys. Rev., 56(10), pp. 978-982, 1939, DOI: 10.1103/PhysRev.56.978.
[16] Kittel, C., Introduction to solid state physics, 8th edn. University of California, Berkeley, USA, 2005.
[17] Cuervo-Farfán, J., Olaya, J.J., Vera-López, E., Landínez-Téllez, D.A. and Roa-Rojas, J., Impedance spectroscopy and structural properties of the perovskite-like $Sn(Ba,Sr)_{O3}$ stagnate, Physica B 407(16), pp. 3089-3092, 2012, DOI: 10.1016/j.physb.2011.12.032.
[18] Ortiz-Diaz, O., Rodríguez, J.A., Fajardo, F., Landínez-Téllez, D.A. and Roa-Rojas, J., Electronic and structural properties of Sr_2YSbO_6, Physica B 398(2), pp. 248-251, 2007. DOI: 10.1016/j.physb.2007.04.077.

R. Cardona, received as Physicist in 1980, MSc. degree in Physics in 1997 and PhD degree in Physics in 2003, all of them from the Universidad Nacional de Colombia, Bogotá, Colombia. Is associated professor in Physics Department, of the Universidad Nacional de Colombia,, Bogotá. Research issues: electronic structure, perovskite materials, semiconductors.
ORCID: 0000-0002-4003-9116.

D.A. Landínez-Téllez, received as Physicist in 1991 from the Universidad Industrial de Santander, Bucaramanga, Colombia, MSc degree in Physics in 1994 form the Universidade de Brasília, Brasília, Brasil, PhD degree in Physics in 1999 from the Universidade Federal de Pernambuco, Recife, Brasil. Is associated professor in Physics Department, Universidad Nacional de Colombia, Bogotá, Colombia. Research issues: electronic structure, perovskite materials, crystallography, superconductivity, magnetism, synthesis of ceramic materials, ferroelectricity, multiferroics materials and devices.
ORCID: 0000-0001-7108-617X.

J. Roa-Rojas, received as Physicist in 1991 from the Universidad Industrial de Santander, Bucaramanga, Colombia, MSc degree in physics in 1994 from the Universidade de Brasília, Brasília, Brasil, PhD degree in physics in 1999 from the Universidade Federal do Rio Grande do Sul, Brasil. Is titular professor in Physics Department, Universidad Nacional de Colombia, Bogotá, Colombia. Research issues: electronic structure, perovskite materials, crystallography, superconductivity, magnetism, synthesis of ceramic materials, ferroelectricity, multiferroics materials and devices.
ORCID: 0000-0002-5080-8492.

UNIVERSIDAD NACIONAL DE COLOMBIA
SEDE MEDELLÍN
FACULTAD DE MINAS

Área Curricular de Ingeniería
Geológica e Ingeniería de Minas y Metalurgia

Oferta de Posgrados

Especialización en Materiales y Procesos
Maestría en Ingeniería - Materiales y Procesos
Maestría en Ingeniería - Recursos Minerales
Doctorado en Ingeniería - Ciencia y Tecnología de Materiales

Mayor información:

E-mail: acgeomin_med@unal.edu.co
Teléfono: (57-4) 425 53 68